

**TITLE**

**Folding is Not Required for Bilayer Insertion: Replica Exchange Simulations of an  $\alpha$ -Helical Peptide with an Explicit Lipid Bilayer**

**AUTHORS****Hugh Nymeyer**

Theoretical Biology & Biophysics Group, T-10  
MS K710, T-10  
Los Alamos National Laboratory  
Los Alamos, NM 87545

PHONE: 505-660-5171  
FAX: 505-665-3943  
EMAIL: hugh@lanl.gov

**Thomas B. Woolf**

Depts of Physiology and of Biophysics  
Johns Hopkins University, School of Medicine  
725 N. Wolfe St.  
Baltimore, MD 21205

PHONE: 410-614-2643  
FAX: 410-614-4436  
EMAIL: woolf@groucho.med.jhmi.edu

**Angel E. Garcia (*Corresponding Author*)**

Theoretical Biology & Biophysics Group, T-10  
MS K710, T-10  
Los Alamos National Laboratory  
Los Alamos, NM 87545

PHONE: 505-665-5341  
FAX: 505-665-3943  
EMAIL: axg@lanl.gov

**SHORT TITLE****Folding is not Required for Bilayer Insertion****KEYWORDS**

Four Stage Model; Replica Exchange Molecular Dynamics; WALP;

## ABSTRACT

We implement the replica exchange molecular dynamics algorithm to study the interactions of a model peptide (WALP-16) with an explicitly represented DPPC membrane bilayer. We observe the spontaneous, unbiased insertion of WALP-16 into the DPPC bilayer and its folding into an  $\alpha$ -helix with a trans-bilayer orientation. We observe that the insertion of the peptide into the DPPC bilayer precedes secondary structure formation. Although the peptide has some propensity to form a partially helical structure in the interfacial region of the DPPC/water system, this state is not a productive intermediate but rather an off-pathway trap for WALP-16 insertion. Equilibrium simulations show that the observed insertion/folding pathway mirrors the potential of mean force (PMF). Calculation of the enthalpic and entropic contributions to this PMF show that the surface bound conformation of WALP-16 is significantly lower in energy than other conformations, and that the insertion of WALP-16 into the bilayer without regular secondary structure is enthalpically unfavorable by 5-10 kcal/mol/residue. The observed insertion/folding pathway disagrees with the dominant conceptual model<sup>1-3</sup>, which is that a surface bound helix is an obligatory intermediate for the insertion of  $\alpha$ -helical peptides into lipid bilayers. In our simulations, the observed insertion/folding pathway is favored because of a large (> 100 kcal/mol) increase in system entropy that occurs when the unstructured WALP-16 peptide enters the lipid bilayer interior. The insertion/folding pathway that is lowest in free energy depends sensitively on the near cancellation of large enthalpic and entropic terms. This suggests that intrinsic membrane peptides may have a

**diversity of insertion/folding behaviors depending on the exact system of peptide and lipid under consideration.**

Membranes and membrane proteins are dynamically active systems involved in essential biological processes. Whole genome analysis indicates that 20-30% of all open reading frames code for membrane spanning  $\alpha$ -helical bundle proteins<sup>4,5</sup>. Proteins with  $\beta$ -barrel architectures (e.g. porins) are coded for by several percent of the open reading frames in bacteria<sup>6</sup> and an unknown fraction in eukaryotic organisms. Many other proteins involved in cell-cell adhesion, immune recognition, and signal transduction also have single  $\alpha$ -helical membrane spanning domains<sup>7</sup>. Because of difficulties in isolating, purifying, and crystallizing membrane proteins, only about 82 unique intrinsic membrane protein structures are known<sup>3,8</sup> at atomic resolution compared with the thousands of globular proteins that have been solved<sup>9</sup>. Consequently, the protein-protein and protein-lipid interactions that stabilize intrinsic membrane proteins are not as well understood as the interactions that stabilize globular proteins. Prediction of membrane protein structure, of membrane protein folding, and of membrane protein dynamics is limited by our understanding of these protein-lipid interactions and lipid dynamics<sup>10</sup>.

Because of these difficulties, model systems have been instrumental for understanding the general principles governing membrane protein structure and dynamics. An important model system has been the WALP series of peptides, which have an alternating, variable length alanine/leucine core flanked on both termini by two tryptophan residues<sup>11-13</sup>. These peptides have been demonstrated to form trans-membrane  $\alpha$ -helices by CD<sup>11</sup>, NMR<sup>11,14,15</sup>, UV-Vis spectroscopy<sup>14</sup>, transmission and atomic force microscopy<sup>16,17</sup>, and mass spectrometry<sup>18-20</sup>. The compensatory changes in lipid structure induced by WALP peptides have also been studied via NM<sup>11,20-26</sup>, electron spin resonance<sup>21,22</sup>,

microscopy<sup>24</sup>, x-ray diffraction<sup>27</sup>, and calorimetry<sup>25</sup>. These experimental studies have been complemented by molecular dynamics calculations, which have attempted to discern what lipid and peptide structural adjustments might occur for different length WALPs and different bilayer settings<sup>28</sup>.

In this paper we report all-atom simulations of the interactions of a 16 residue WALP peptide with a solvated DPPC bilayer. Our simulations show the spontaneous insertion and folding of this WALP-16 peptide into the DPPC bilayer. These simulations are the first to show the unbiased, spontaneous insertion and folding of a hydrophobic peptide into an explicitly represented lipid bilayer. The spontaneous insertion and folding of peptides into trans-bilayer configurations is difficult to observe, because most membrane spanning peptides are highly hydrophobic and thus prone to aggregation. To our knowledge only three experimental kinetic studies of spontaneous peptide insertion processes exist<sup>29-31</sup>. Although no kinetic measurements of WALP insertion have been made, generic models of peptide insertion and folding have been constructed based on thermodynamic arguments<sup>1-3</sup>. Our simulated insertion does not agree with these models, suggesting that other previously discounted thermodynamic effects in the lipid component may alter the insertion process in some peptide/bilayer systems.

Our simulations have been conducted using 1024 processors on the Q-machine, a parallel computer at Los Alamos National Laboratory which at the time of this simulation is ranked as the third fastest in the world<sup>32</sup>. We have implemented a replica exchange (parallel tempering) molecular dynamics algorithm<sup>8</sup> on this machine. Replica exchange algorithms<sup>33-37</sup> were developed to study glassy systems with long relaxation times and are widely used in the context of protein folding<sup>38-40</sup> (reviewed by Nymeyer et al.<sup>41</sup>). In these

methods, multiple copies or replicas of the same system are simulated in parallel at different temperatures, and temperatures are periodically exchanged between two replicas in a manner that preserves detailed balance. These algorithms speed equilibration by a large factor (perhaps 100x or more)<sup>42-44</sup> and enable us to observe insertion of a WALP peptide while simultaneously computing the equilibrium properties of the WALP/DPPC bilayer system.

As described in the methods section, we run three simulations. The first simulation begins with the peptide in a water solvated conformation. This simulation shows WALP spontaneously moving into conformations in which it is anchored into the bilayer. The second simulation starts with the peptide in an anchored conformation. This simulation shows four separate events in which WALP spontaneously inserts completely into the bilayer and forms  $\alpha$ -helical secondary structure. The third simulation, which begins with the peptide inserted completely in the bilayer, is used to generate an equilibrium ensemble of WALP/DPPC conformations and measure the changes in thermodynamic quantities as a function of peptide structure and location in the bilayer.

The first two simulations suggest an insertion mechanism for WALP with three steps. In the first step, the peptides move into a membrane-anchored conformation. In this conformation, the peptide has inserted one or more of its Trp residues into the bilayer below the phosphate groups. These Trp residues anchor the peptide to the bilayer, although the peptide itself is still mostly water solvated. In the second step, the peptides insert into the lipid bilayer in an unstructured state, occupying the volume exposed in the lipid due to fluctuations of the lipid chains. In the third step these peptides form a helical nucleus, from

which the whole  $\alpha$ -helix rapidly forms. This helix orients roughly normal to the bilayer surface. These basic steps are observed in all the WALP peptides that inserted and folded. No WALP's were observed to insert directly from a surface bound helical conformation.

One of the observed insertion trajectories is shown in figure 1. Steps in the trajectory are shown along with a projection of the trajectory onto the plane spanned by distance of the WALP from the central bilayer plane and helical content of the WALP peptide. This trajectory is superimposed upon the potential of mean force (PMF). The trajectory of the inserted peptides mirrors the underlying potential of mean force determined in equilibrium.

The PMF at this temperature has three dominant basins of attraction. In the first basin, the peptide is mostly water solvated and non-helical but possibly anchored via one or more Trp residues into the membrane. In the second basin, the peptide is located in the bilayer interface and non-helical. This basin is a mixture of states in which the peptide is lying approximately in the plane of the interface and states in which the peptide is approximately normal to the interface. In the third basin, the peptide is helical and inserted in the membrane. The principal barrier to folding occurs during nucleation of the peptide in the center of the lipid bilayer. Although our PMF is shown for temperatures greater than the experimental conditions, extrapolation to lower temperatures does not appear to alter the insertion mechanism; however, the barrier to insertion does increase with decreasing temperature.

By fitting the temperature variation of our PMF, we have estimated the enthalpic and entropic changes of our system with peptide structure and position. These results (Figure 2) agree with the known thermodynamics of peptides interacting with lipid bilayers. In



particular, we find that the insertion of the WALP-16 peptide into the DPPC bilayer in a largely unstructured state entails a significant enthalpic penalty of between 5-10 kcal/mol per residue. This is in agreement with calculations<sup>45</sup> and measurements on model compounds<sup>46,47</sup> that provide estimates of an enthalpic backbone desolvation penalty of 6-8 kcal/mol per residue. As expected, the enthalpy decreases sharply by nearly the same amount with the growth of hydrogen bonds along the  $\alpha$ -helix. Although helix formation in water is generally enthalpically favored, helix formation followed by insertion may be less enthalpically favorable or even unfavorable, since hydrogen bonds in a fully formed  $\alpha$ -helix retain some residual electrostatic interaction with the surrounding solvent<sup>48</sup>.

Waters bound to the WALP may play an important role in stabilizing the peptide when inserted in the bilayer. Although we have prevented waters from penetrating to the center of the bilayer via a weak mean-field potential (see Methods for details), we still observe a significant amount of water bound to the WALP backbone prior to  $\alpha$ -helix formation (see figure 4). Bound waters are certain to make insertion of the unfolded peptide more favorable than would be expected based on complete backbone desolvation. Figure 2 indicates that initially, insertion of the WALP is not strongly disfavored by enthalpy, presumably due to the presence of these bound waters.

From figure 2 we see that the surface bound partly helical conformations of the peptide are exceptionally low in energy. There are few experimental measurements of enthalpy changes upon the binding of small molecules to lipid bilayers. Jacobs and White<sup>2</sup> found negligible enthalpy changes upon binding of the small peptides Ala-X-Ala-O-*tert*-butyl (X = Leu, Phe, Trp) to DMPC vesicles. Similar results were found the COX IV

peptide<sup>49</sup> and for several Trp derivatives<sup>50</sup>. In contrast, many aromatic amphiphiles have negative enthalpy changes upon binding to lipid bilayers<sup>3,51-53</sup>. DeVido et al.<sup>54</sup> suggest that negative enthalpic changes are generic for spontaneous binding of small molecules to ordered lipid chain phases. Figure 5 indicates that a strong Coulombic interaction can exist between the TRP residues which cap WALP and the phosphatidylcholine groups. This strong interaction is consistent with the experiments and statistical studies<sup>55</sup> that suggest favorable enthalpic interactions between Trp side chains and the DPPC/water interface. It is also expected that  $\alpha$ -helical hydrogen bonds will be more enthalpically favorable in the interface, because its effective dielectric constant is reduced from that of bulk water (probably to an  $\epsilon$  of  $\approx 18$ )<sup>3,56,57</sup>.

Although the partially folded helical surface bound conformations of WALP are low in energy, no passage directly these conformations to a trans-membrane helix is observed, suggesting that the surface bound state is acting more as an off-pathway trap than an intermediate for WALP insertion. Peptides other than WALP may be more stabilized as interfacial helices. Stronger stabilization of interfacial helices should favor insertion directly from a surface bound helical conformation.

The observed insertion behavior and the equilibrium potential of mean force disagree with the accepted hypothesis about the spontaneous insertion of peptides into lipid bilayers<sup>1-3</sup>. The accepted hypothesis, known as the four stage model (figure 3), posits that insertion into the membrane interior should occur only after significant secondary structure has already formed. This conclusion is based on calculations<sup>45</sup> and measurements<sup>46-47</sup> using bulk hydrophobic solvents, which show that the insertion of an unstructured peptide into

the lipid interior will entail a high enthalpic cost due to the desolvation of the peptide backbone. This desolvation penalty is mostly absent in regularly structured peptides, because the backbone is already desolvated to a large extent, and the peptide hydrogen bond donors and acceptors are satisfied internally.

Our simulations are in agreement with the calculations and measurements suggesting a large penalty for backbone desolvation. However, our simulations also show that entropic changes are strong enough to overcome this desolvation penalty. No reliable estimates or measurements of the entropic changes due to the insertion of an unstructured peptide into a lipid bilayer exist to which we may compare our simulations; however, the observed entropic compensation effect is too large to be purely a simulation artifact.

Our molecular dynamics simulation results depend significantly on the force field used for the protein and the lipid and on the simulation conditions such as constant volume, constant cross sectional surface area, and system size. For example, we observe a transition to an ordered, gel like tilted phase for the lipid below 400K, while the transition should occur at 314 K. However, our simulations provide a molecular view of the folding of a transmembrane  $\alpha$ -helix within an explicit lipid bilayer and suggest that the insertion and folding of peptides into lipid bilayers might be more complex than suggested. Simulations of peptides that are known to co-exist in the water and lipid phases<sup>58,59</sup> are under way. We expect our simulations to motivate experimentation of the time resolved kinetics of the insertion and folding of peptides in membranes.

In conclusion, our simulations provide a molecular view of the folding of a transmembrane  $\alpha$ -helix within an explicit lipid bilayer. Our results show that the folding

process might be more complex and subtle than suggested by the four stage model. In particular, we observe large entropic changes in the system that may make insertion of peptides into the bilayer prior to secondary structure formation favorable. The composition of the peptide and lipid are certain to modulate the large enthalpic and entropic terms driving insertion, making insertion mechanisms more variable than have been suggested by the four stage model. In this regard we suggest that membrane proteins, like globular proteins, may have multiple folding routes best described as motion on a multi-dimensional free energy surface<sup>60,61</sup>. More experimental studies of the folding pathways for  $\alpha$ -helical monomers and dimers would be useful to further understand the molecular interplay that occur within the heterogenous solvation setting of the membrane bilayer and its associated waters.

## Methods

### Initial conditions

The starting point of our simulations is a fully solvated WALP-16 peptide [CHO-ALA-TRP<sub>2</sub>-(LEU-ALA)<sub>5</sub>-TRP<sub>2</sub>-ALA-Ethanolamine] with 1048 TIP3P waters and a bilayer with 18 DPPC molecules in each monolayer. The initial conditions of the lipid were derived from previous simulations of the WALP-16 in a DPPC bilayer<sup>8</sup>. The WALP-16 peptide was placed initially into an unfolded water-solvated conformation with its long axis approximately horizontal to the membrane plane. The surface area per lipid in this initial conformation is 68 Å<sup>2</sup>. The surface area per lipid in pure DPPC bilayers has been measured<sup>62</sup> to be 64 Å<sup>2</sup>; however, the surface area for a mixed DPPC/WALP system is not

accurately known. We assumed a constant surface area throughout the insertion process. This surface area was chosen to match the result of another DPPC/WALP simulation performed with the same force-field<sup>5</sup>.

## Simulations

Simulations were carried out via a modified version of the CHARMM (version 28) program<sup>63</sup>. The force-field/energy function was the CHARMM22 all-atom force-field of Schlenkrich et al.<sup>64,65</sup>.

The initial simulation was a 1ns replica exchange simulation using 38 replicas of the system with temperatures exponentially spaced from 350-505.8K. This was followed by a 1.6ns simulation involving 64 replicas exponentially spaced from 350K to 800K, where the simulation continued from a membrane anchored conformation obtained at the end of the initial 1ns simulation. Our lowest temperature is above the experimentally known phase transition of the DPPC bilayer (~314K).

For  $N$  replicas, exchanges are attempted between  $N^2$  randomly chosen pairs of replicas at intervals of 250 integration steps. Integration steps are 2fs for the first 1.4 ns; 0.8fs for the next 200ps; and 1fs for the remainder. All bonds involving water are fixed for the first 1.6ns; all bonds involving hydrogen are fixed for the last 1ns. PME is used for the electrostatics with a 32x32x64 grid with fourth order spline interpolation, a 4Å width Gaussian screening charge, and a 10-12Å switching function on the direct interaction. The ensemble is NVT in a 35x35x72.75Å box with a Nose-Hoover thermostat with a mass of 500 a.u..

A planar restraint is placed on the average position of the C<sub>2</sub> atom in each DPPC monolayer to maintain the membrane structure at high temperature. The minima are at +18.3555Å and -18.2203Å. The restraining potential is zero within 0.25Å of the minimum and quadratic with a 10kcal/mol/Å<sup>2</sup> force constant outside this region. A quadratic restraint of the form 0.2kcal/mol-Å<sup>2</sup> × D<sup>2</sup> × (D<sup>2</sup>-2.25Å<sup>2</sup>) applies to the water oxygens where D=z-25Å for z>0 and D=z+25Å for z<0. The effect of these constraints on the equilibrium properties of the lipid appears to be minimal since the calculated surface area tension of 35 dyn/cm at low T is consistent with the values reported for the force field used in our calculations<sup>66</sup>. The calculated surface tension decreases as T increases and becomes negative at T> 430 K.

The equilibrium simulation has identical settings. All replicas are started inserted but are non-helical. Step size is 0.8fs for the first 200ps with only the waters held rigid and 1fs for the remainder with all bonds involving hydrogen held fixed. Total simulation time is 3.5ns per replica. The final 1.5ns is used for analysis.

## Analysis

The potential of mean force was computed for each temperature as  $-RT\ln(N)$ , where N is the number of counts per bin at temperature T in Kelvin, and R is the ideal gas constant in units of kcal/mol/K. The ordinate is the absolute value of the Z-coordinate of the WALP-16 center of mass with origin placed at the bilayer center. The abscissa is the number of  $\alpha$ -helical hydrogen bonds determined with a 3.5Å cutoff on the hydrogen-oxygen distance and a 90 degree cutoff on the angle between the C-O and H-N vectors.

All points in the potential of mean force plane with counts at 7 or more temperatures were used to determine the thermodynamic formula:

$$\Delta G = \Delta E - T\Delta S$$

$$\Delta E = \Delta E_0 + \int_{T_0}^T \Delta C_v dT'$$

$$\Delta S = \Delta S_0 + \int_{T_0}^T \frac{\Delta C_v}{T'} dT'$$

$$\Delta C_v = \Delta C_{v_0} + (d\Delta C_v / dT)_0 (T - T_0)$$

where the four parameters are: relative energy  $\Delta E_0$  at temperature  $T_0$ , relative entropy  $\Delta S_0$ , relative heat capacity  $\Delta C_{v_0}$ , and the change in relative heat capacity with temperature  $(d\Delta C_v / dT)_0$ . Contours of  $\Delta G$  are shown in figure 1. Contours of  $\Delta E$  and  $-T\Delta S$  are shown in figure 2. Points sampled at fewer than 7 temperatures are not shown.

### **Acknowledgements:**

We thank A. Ladokhin, R. W. Pastor and S.H. White for enlightening discussions. This work was supported by the US DOE by LDRD project. Computer facilities were provided by Los Alamos Institutional Computing. In particular we thank D. Dawson, H. Marshall, M. Vigil, and C. Wampler for their assistance in porting code and using the Q machine at Los Alamos.

**Bibliography:**

1. Popot JL, Engelman, DM. Membrane-protein folding and oligomerization: the 2-stage model. *Biochemistry* 1990; 29: 4031-4037.
2. Jacobs RE, White SH. The nature of the hydrophobic binding of small peptides at the bilayer interface: implications for the insertion of transbilayer helices. *Biochemistry* 1989; 28: 3421-3437.
3. White SH, Wimley WC. Membrane protein folding and stability: physical principles. *Annu Rev Biophys Biomol Struct* 1999; 28: 319-365.
4. Boyd D, Schierle C, Beckwith J. How many membrane proteins are there? *Prot Sci* 1998; 7: 201-205.
5. Wallin E, Von Heijne G. Genome-wide analysis of integral membrane proteins from eubacterial, archaean, and eukaryotic organisms. *Prot Sci* 1998; 7: 1029-1038.
6. Wimley WC. Toward genomic identification of  $\beta$ -barrel membrane proteins: compositions and architecture of known structure. *Prot Sci* 2002; 11: 301-312.
7. Landoltmarcorena C, Williams KA, Deber CM, Reithmeier RAF. Nonrandom distribution of amino acids in the transmembrane segments of human type-I single span membrane-proteins. *J Mol Biol* 1993; 229: 602-608.
8. White S. 2004 May 2. Membrane proteins of known 3D structure. <[http://blanco.biomol.uci.edu/Membrane\\_Proteins\\_xtal.html](http://blanco.biomol.uci.edu/Membrane_Proteins_xtal.html)> Accessed 2004 May 10.
9. Berman HM, Westbrook J, Feng Z, Gilliland G, et al. The Protein Data Bank. *Nucleic Acids Res* 2000; 28: 235-242. (See also <http://www.rcsb.org/pdb>)
10. Popot JL, Engelman DM. Helical membrane protein folding, stability, and evolution. *Annu Rev Biochem* 2000; 69: 881-922.



11. Killian JA et al. Induction of nonbilayer structure in diacylphosphatidylcholine model membranes by transmembrane  $\alpha$ -helical peptides: importance of hydrophobic mismatch and proposed role of tryptophans. *Biochemistry* 1996; 35: 1037-1045.
12. Killian JA. Hydrophobic mismatch between proteins and lipids in membranes. *Biochim Biophys Acta-Rev Biomembr* 1998; 1376: 401-416.
13. De Planque MRR, Killian JA. Protein-lipid interactions studied with designed transmembrane peptides: role of hydrophobic matching and interfacial anchoring (Review). *Mol Membr Biol* 2003; 20: 271-284.
14. de Planque MRR et al. Sensitivity of single membrane-spanning  $\alpha$ -helical peptides to hydrophobic mismatch with a lipid bilayer: effects on backbone structure, orientation, and extent of membrane incorporation. *Biochemistry* 2001; 40: 5000-5010.
15. van der Wel PCA et al. Geometry and intrinsic tilt of a tryptophan-anchored transmembrane  $\alpha$ -helix determined by  $^2\text{H}$  NMR. *Biophys J* 2002; 83: 1479-1488.
16. Rinia HA et al. Visualization of highly ordered striated domains induced by transmembrane peptides in supported phosphatidylcholine bilayers. *Biochemistry* 2000; 39: 5852-5858.
17. Rinia HA et al. Domain formation in phosphatidylcholine bilayers containing transmembrane peptides: specific effects of flanking residues. *Biochemistry* 2002; 41: 2814-2824.
18. Demmers JAA et al. Electrospray ionization Mass Spectrometry as a tool to analyze hydrogen/deuterium exchange kinetics of transmembrane peptides in lipid bilayers. *Proc Nat'l Acad Sci USA* 2000; 97: 3189-3194.

19. Demmers JAA et al. Interfacial positioning and stability of transmembrane peptides in lipid bilayers studied by combining hydrogen/deuterium exchange and mass spectrometry. *J Biol Chem* 2001; 276: 34501-34508.
20. de Planque MRR et al. Interfacial anchor properties of tryptophan residues in transmembrane peptides can dominate over hydrophobic matching effects in peptide-lipid interactions. *Biochemistry* 2003; 42: 5341-5348.
21. de Planque MRR et al. Influence of lipid/peptide hydrophobic mismatch on the thickness of diacylphosphatidylcholine bilayers. a  $^2\text{H}$  NMR and ESR study using designed transmembrane  $\alpha$ -helical peptides and gramicidin A. *Biochemistry* 1998; 37, 9333-9345.
22. de Planque MRR et al. Different membrane anchoring positions of tryptophan and lysine in synthetic transmembrane  $\alpha$ -helical peptides. *J Biol Chem* 1999; 274: 20839-20846.
23. Morein S et al. The effect of peptide/lipid hydrophobic mismatch on the phase behavior of model membranes mimicking the lipid composition in *Escherichia coli* membranes. *Biophys J* 2000; 78: 2475-2485.
24. de Planque MRR et al. The effects of hydrophobic mismatch between phosphatidylcholine bilayers and transmembrane  $\alpha$ -helical peptides depend on the nature of interfacially exposed aromatic and charged residues. *Biochemistry* 2002; 41: 8396-8404.
25. Morein S, Killian JA, Sperotto MM. Characterization of the thermotropic behavior and lateral organization of lipid-peptide mixtures by a combined experimental and theoretical approach: effects of hydrophobic mismatch and role of flanking residues. *Biophys J* 2002; 82: 1405-1417.
26. Morein S et al. Influence of membrane-spanning  $\alpha$ -helical peptides on the phase behavior of the dioleoylphosphatidylcholine/water system. *Biophys J* 1997; 73: 3078-3088.

27. Weiss TM et al. Hydrophobic mismatch between helices and lipid bilayers. *Biophys J* 2003; 84: 379-385.
28. Petrache HI, Zuckerman DM, Sachs JN, Killian JA, Koeppe RE, Woolf TB. Hydrophobic matching mechanism investigated by molecular dynamics simulations. *Langmuir* 2002; 18: 1340-1351.
29. Hunt JF, Rath P, Rothschild KJ, Engelman DM. Spontaneous, pH-dependent membrane insertion of a transbilayer  $\alpha$ -helix. *Biochemistry* 1997; 36: 15177-15192.
30. Meijbert W, Booth PJ. The activation energy for insertion of transmembrane  $\alpha$ -helices is dependent on membrane composition. *J Mol Biol* 2002; 319: 839-853.
31. Yano Y, Matsuzaki K. Membrane insertion and dissociation processes of a model transmembrane helix. *Biochemistry* 2002; 41: 12407-12413.
32. Dongarra JJ, Meuer HW, Strohmaier E. TOP500 supercomputer sites. *Supercomputer* 1997; 13: 89-120. (see also <http://www.top500.org>)
33. Sugita Y, Okamoto Y. Replica-exchange molecular dynamics method for protein folding. *Chem Phys Lett* 1999; 314: 141-151.
34. Swendsen R, Wang J. *Phys Rev Lett* 1986; 57: 2607-2609.
35. Marinari E, Parisi G. Simulated tempering - a new monte-carlo scheme. *Europhys Lett* 1992; 19: 451-458.
36. Geyer C, Thompson E. Annealing Markov-chain monte-carlo with applications to ancestral inference. *J Am Stat Assoc* 1995; 90: 909-920.
37. Hukushima K, Nemoto K. Exchange monte-carlo simulations and application to spin glass simulations. *J Phys Soc Japan* 1996; 65: 1604-1608.

38. Hansmann, U. Parallel tempering algorithm for conformational studies of biological molecules. *Chem Phys Lett* 1997; 281: 140-150.
39. Garcia AE, Sanbonmatsu KY. Exploring the energy landscape of a  $\beta$  hairpin in explicit solvent. *Prot Struct Funct Genet* 2001; 42: 345-354.
40. Sanbonmatsu, K. Y. & Garcia, A. E. Structure of met-enkephalin in explicit aqueous solutions using replica exchange molecular dynamics. *Prot Struct Funct Genet* 2002; 46, 225-234.
41. Nymeyer H, Gnanakaran S, Garcia AE. Atomic simulations of protein folding, using the replica exchange algorithm. *Methods Enzymol* 2004; 383: 119-149.
42. Garcia AE, Sanbonmatsu KY. Alpha-helical stabilization by side chain shielding of hydrogen bonds. *Proc Nat'l Acad Sci USA* 2002; 99: 2782-2787.
43. Yamamoto R, Kob W. Replica-exchange molecular dynamics simulation for supercooled liquids. *Phys Rev E* 2000; 61: 5473-5476.
44. Bedrow D, Smith GD. Exploration of conformational phase space in polymer melts: a comparison of parallel tempering and conventional molecular dynamics simulations. *J Chem Phys* 2001; 115: 1121-1124.
45. Ben-Tal N, Sitkoff D, Topol IA, Yang A-S, et al. Free energy of amide hydrogen bond formation in vacuum, in water, and in liquid alkane solution. *J Phys Chem B* 1997; 101: 450-457.
46. Roseman MA. Hydrophobicity of the peptide C=O  $\cdots$  H-N hydrogen-bonded group. *J Mol Biol* 1998; 201: 621-623.
47. Wimley WC, Creamer TP, White SH. Solvation energies of amino acid side chains and backbone in a family of host-guest pentapeptides. *Biochemistry* 1996; 35: 5109-5124.

48. Ben-Tal N, Ben-Shaul A, Nicholls A, Honig B. Free-energy determinants of  $\alpha$ -helix insertion into lipid bilayers. *Biophys J* 1996; 70: 1803-1812.
49. Russell CJ, Thorgeirsson TE, Shin Y-K. Temperature dependence of polypeptide partitioning between water and phospholipid bilayers. *Biochemistry* 1996; 35: 9526-9532.
50. Jain MK, Rogers J, Simpson L, Gierash LM. Effect of tryptophan derivatives on the phase properties of bilayers. *Biochim Biophys Acta* 1985; 816: 153-162.
51. Seelig J, Ganz P. Nonclassical hydrophobic effect in membrane binding equilibria. *Biochemistry* 1991; 30: 9354-9359.
52. Katzer M, Stillwell W. Partitioning of ABA into bilayers of di-saturated phosphatidylcholines as measured by DSC. *Biophys J* 2003; 84: 314-325.
53. Wimley WC, White SH. Membrane partitioning: distinguishing bilayer effects from the hydrophobic effect. *Biochemistry* 1993; 32: 6307-6312.
54. DeVido DR, Dorsey JG, Chan HS, Dill KA. Oil/water partitioning has a different thermodynamic signature when the oil solvent chains are aligned than when they are amorphous. *J Phys Chem B* 1998; 102: 7272-7279.
55. Yau WM, Wimley WC, Gawrisch K, White SH. The preference of tryptophan for membrane interfaces. *Biochemistry* 1998; 37: 14713-14718.
56. Wimley WC, White SH. Experimentally determined hydrophobicity scale for proteins at membrane interfaces. *Nat Struct Biol* 1996; 3: 842-848.
57. Wimley WC, Gawrisch K, Creamer TP, White SH. A direct measurement of salt-bridge solvation energies using a peptide model system: implications for protein stability. *Proc Nat'l Acad Sci USA* 1996; 93: 2985-2990.

58. Ladokhin AS, Legmann R, Collier RJ, White SH. Reversible refolding of the diphtheria toxin T-domain on lipid membranes. *Biochemistry* 2004; 43: 7451-7458.
59. Ladokhin AS, White SH. Interfacial folding and membrane insertion of a designed helical peptide. *Biochemistry* 2004; 43: 5782-5791.
60. Dill KA, Chan HS. From Levinthal to pathways to funnels. *Nat Struct Biol* 1997; 4: 10-19.
61. Onuchic JN, Nymeyer H, Garcia AE, Chahine J, Socci ND. The energy landscape theory of protein folding: insights into folding mechanisms and scenarios. *Adv Prot Chem* 2000; 53: 87-152.
62. Nagle JF, Tristram-Nagle S. Structure of Lipid Bilayers. *Biochim Biophys Acta – Rev Biomembr* 2000; 1469: 159-195.
63. Brooks, B. R. et al. CHARMM: a program for macromolecular energy, minimization, and dynamics calculations. *J. Comput. Chem.* 1983; 4: 187-217.
64. Schlenkrish M, Brickmann J, MacKerell AD Jr., Karplus M. Empirical potential energy function for phospholipids: criteria for parameter optimization and applications. In: Merz KM, Roux B, editors. *Biological membranes: a molecular perspective from computation and experiment*. Boston: Birkhäuser; 1996. p 31-81.
65. Feller SE, Yin D, Pastor RW, MacKerell AD Jr.. Molecular dynamics simulation of unsaturated lipid bilayers at low hydration: parameterization and comparison with diffraction studies. *Biophys J* 1997; 73: 2269-2279.
66. Feller SE, Pastor RW. Constant surface tension simulations of lipid bilayers: The sensitivity of surface areas and compressibilities. *J Chem Phys* 1999; 111: 1281-1287.

## Figures:

Figure 1: A folding trajectory for the WALP-16 is shown projected onto a two-dimensional surface. The surface shows, with color and contour lines, the relative free energy changes along the changes in hydrogen-bonding of the helix and the z-position of the center-of-mass of the peptide relative to the bilayer center. Color changes occur at 1kcal/mol intervals; solid contour lines are drawn at 2kcal/mol intervals. All folding trajectories followed a similar route with initial stabilization of Trp at the interface followed by insertion and then folding.

Figure 2: Relative changes in enthalpy and entropy show the trade-offs that occur with peptide binding and insertion during the folding process. Colors change at 10kcal/mol intervals; solid contour lines are drawn at 20kcal/mol intervals. In particular, note the gain in enthalpic energy due to initial binding and the 7-11 kcal/mol gain in enthalpy due to hydrogen bond formation during the  $\alpha$ -helical folding within the bilayer interior.

Figure 3: The prevailing conceptual model of helical peptide insertion postulates that all transmembrane domains will fold within the interfacial zone and then insert as a folded domain into the bilayer. The simulation results suggest, at least for this peptide, that the alternative pathway of partial binding at the interface, insertion to the bilayer interior and then folding to an  $\alpha$ -helix can be the preferred route for folding.

Figure 4: The electrostatic interaction energy between WALP and water as a function of WALP center of mass distance from the bilayer central plane (BLACK). Also shown is the number of bound waters versus position (BLUE) determined by counting all waters with an oxygen atom less than 4.0Å in distance from any peptide atom. The bilayer central plane is positioned at  $z = 0$  Å, and the water-lipid interface is near  $z = 20$  Å. Even when the peptide is inserted deep into the membrane, it retains a significant interaction with the aqueous solvent, mostly through the existence of bound waters; consequently, it is not correct to think of the peptide as being completely desolvated even when it is in the center of the bilayer. These two figures were produced by combining the data at many different temperatures. This data was combined by first sorting the electrostatic interaction energy by temperature. At each temperature, the electrostatic energy versus position data was binned into overlapping bins of 5Å width. The average electrostatic energy in each bin was assumed to have a linear variation with temperature. A least squares fit of energy versus temperature was used to determine the best estimate for the average electrostatic energy in each bin at 450K. Any temperature with fewer than ten sampled energies in a bin was not included in the linear fit. The same procedure was followed to compute the number of bound waters versus position. The vertical bars show estimated maximum errors.

Figure 5: The Coulomb interaction energy between the TRP residues and the bilayer as a function of their center of mass positions. The bilayer central plane is



positioned at  $z=0$ , and the water-lipid interface is near  $z = 20$  Å. The TRP residues have a strong electrostatic interaction with the lipid phosphatidylcholine groups that works to stabilize conformations with TRP in this region. The electrostatic interaction energy between TRP and the membrane showed only a small temperature dependence, so all temperature data was combined and binned using a 2Å bin width. The vertical bar is an estimated maximum error.

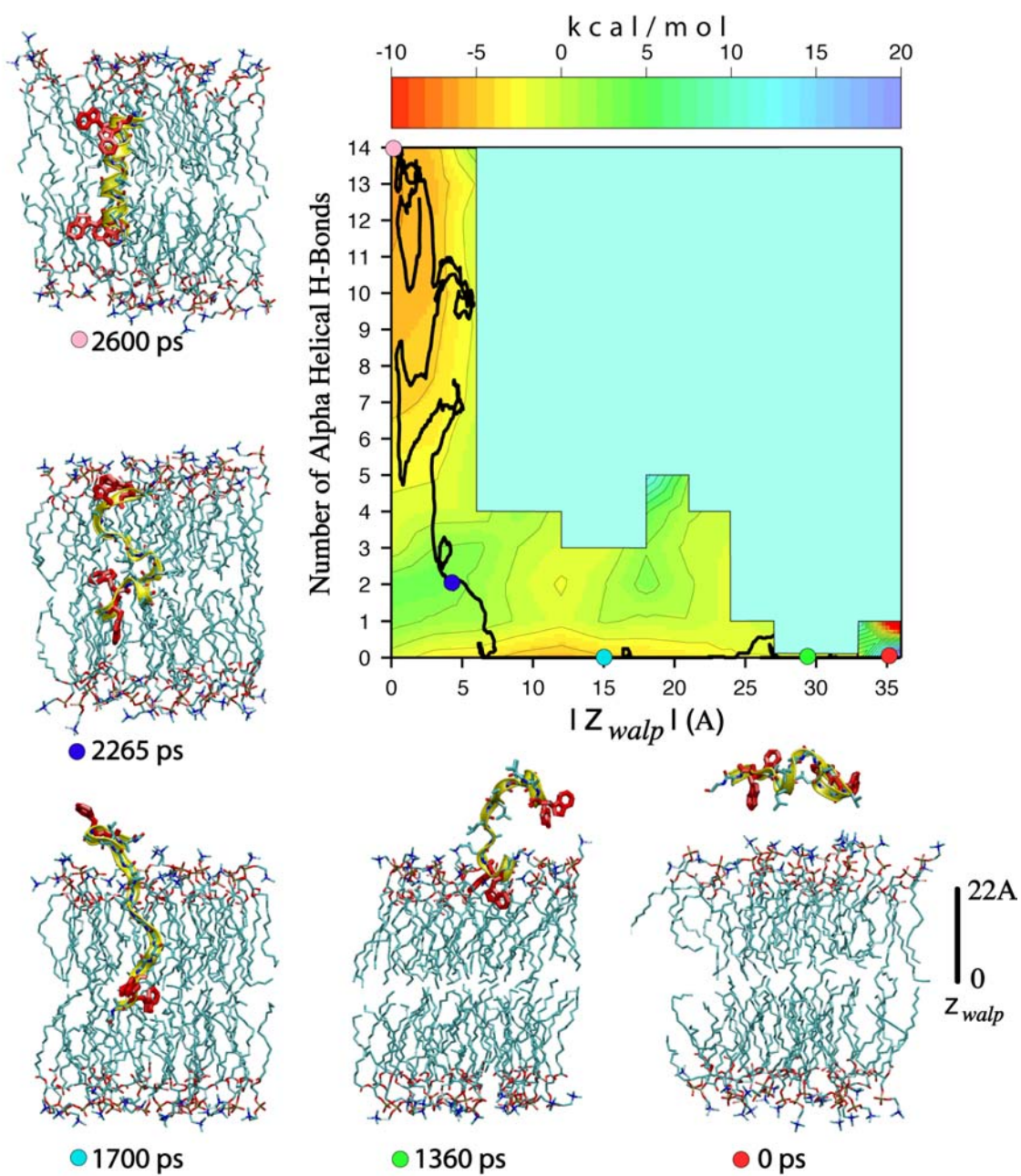


Figure 1.

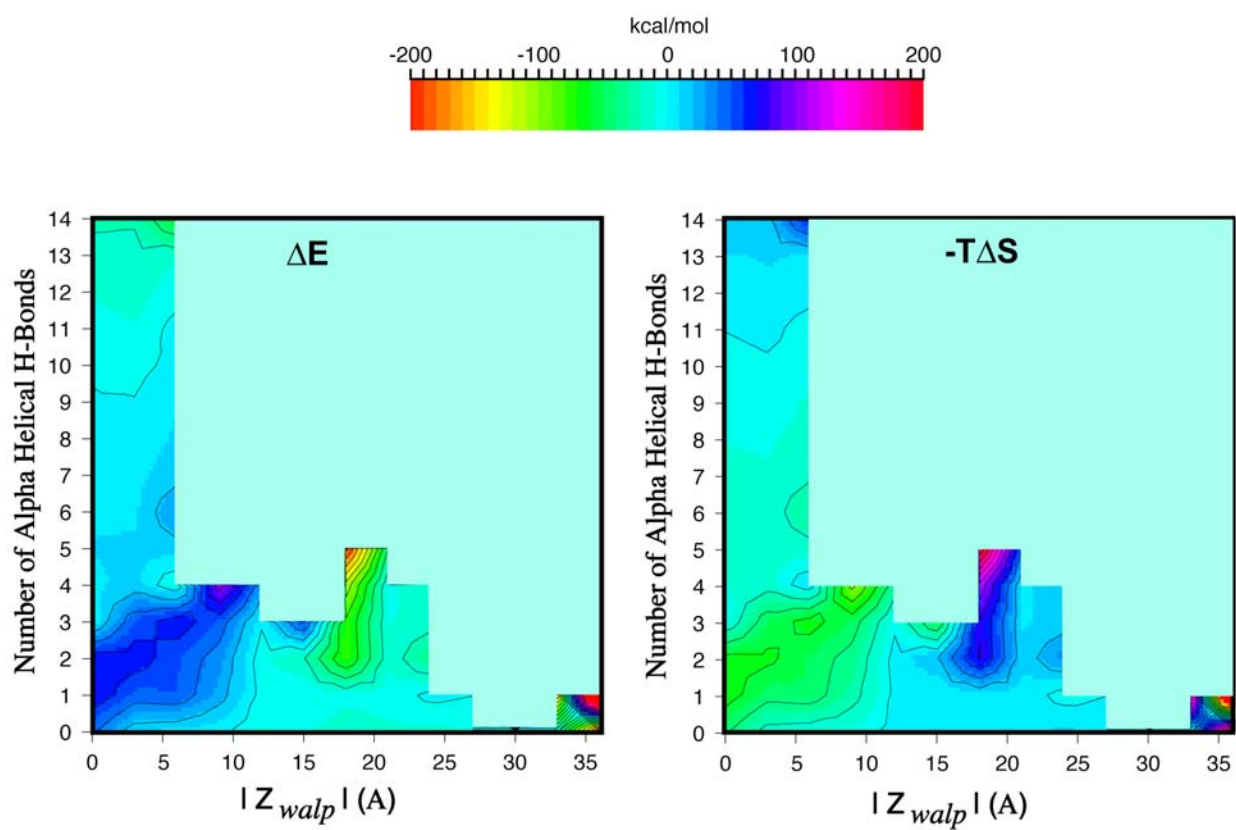


Figure 2.

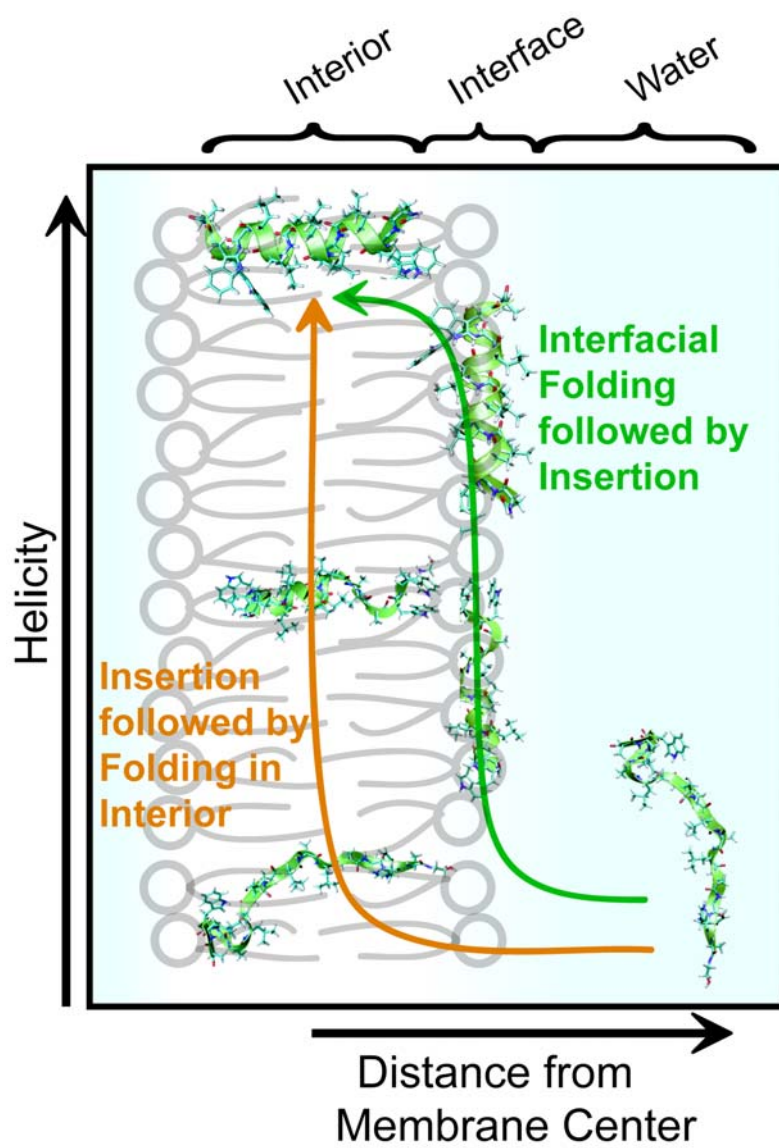


Figure 3.

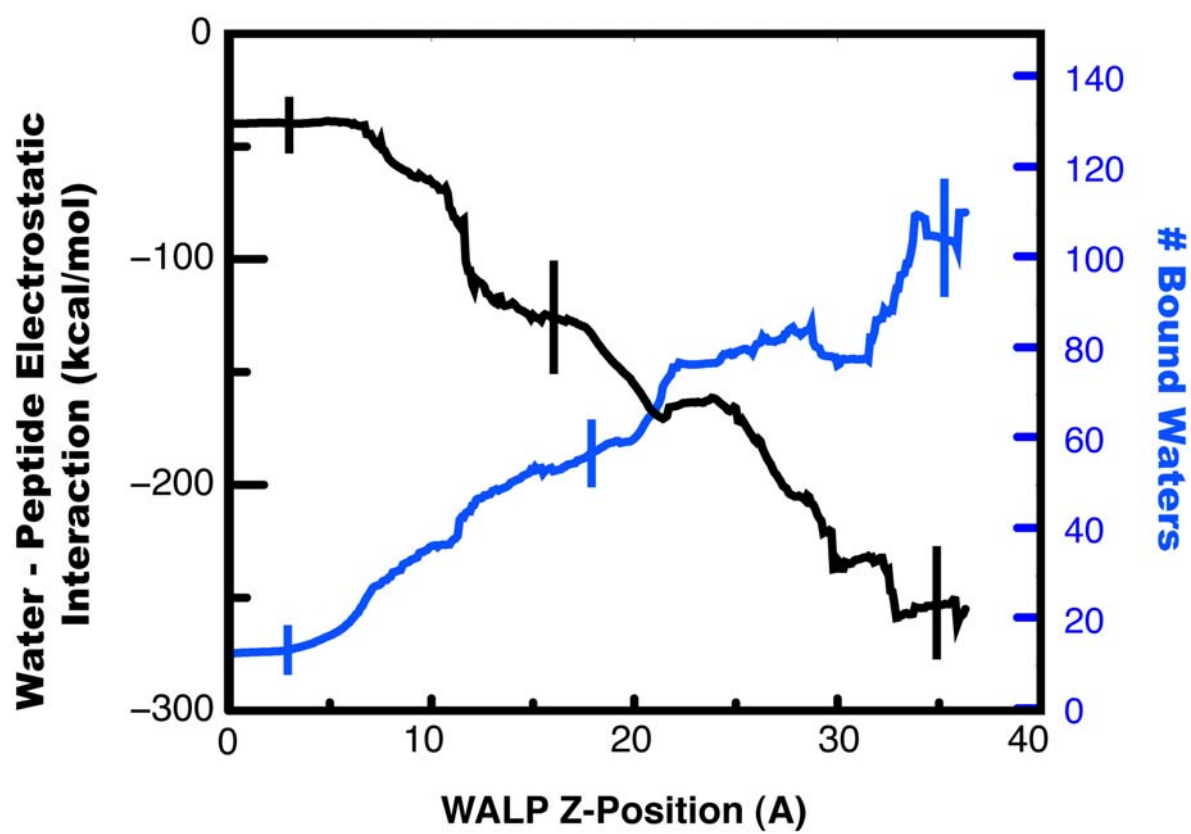


Figure 4.

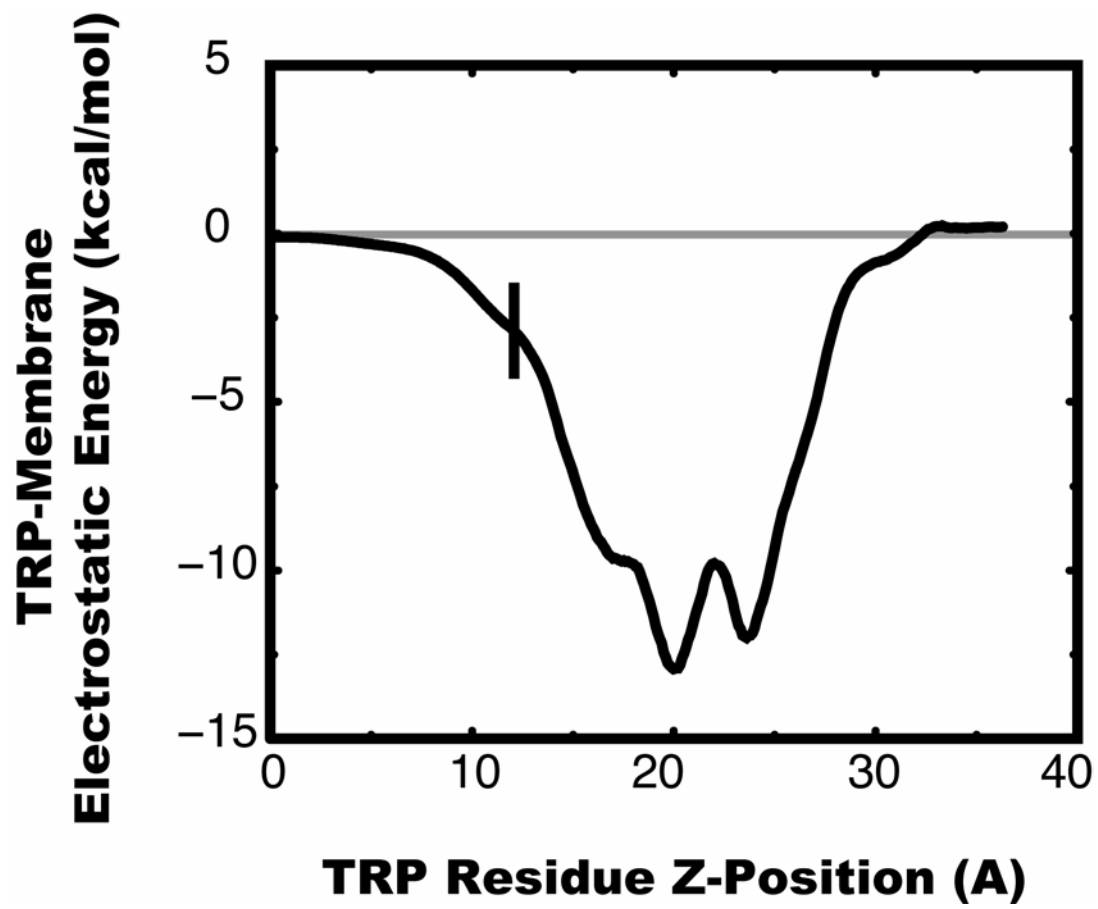


Figure 5.